Adsorption of dyestuff on red perlite: isotherms, kinetics, and thermodynamics

Suchada Sawasdee and Prachart Watcharabundit*

Department of Chemistry, Faculty of Science and Technology, Thepsatri Rajabhat University
*E-mail: ps_neng@hotmail.com

Abstract

Environmental contamination by synthetic dyes has been a serious problem due to their adverse eco-toxicological effects. Recently, there is a growing interest in using low-cost adsorbents to adsorb dyes. In this study, the adsorption experiments were carried out in the batch process to remove a commercial synthetic dye with Lopburi red perlite. The factors affecting the adsorption process, such as pH of dye solution, contact time (5−540 min), initial dye concentration (10−100 mg/L), and temperature (20−40°C) were investigated. The results showed that dye removal reached equilibrium at about 180 min at all temperatures. The Langmuir and Freundlich isotherm models were used to fit the equilibrium data. The better-fitting isotherm model was found to be the Langmuir isotherm at all temperatures. The maximum monolayer adsorption capacity values were 13.70, 14.71, and 16.63 mg/g at 20, 30, and 40°C, respectively. The kinetic adsorption data could be better described by the pseudo-second-order model. Moreover, the thermodynamic study showed that the adsorption was a spontaneous and endothermic process. The results of this study indicated that the red perlite was a good and promising adsorbent for removing dyes.

Keywords: adsorption isotherm, dyestuff, perlite, kinetics, thermodynamics

1. Introduction

Synthetic dyes are widely used in many industries, such as food, cosmetics, and textiles. The presence of pigments can cause damage to living beings in the water. Also, most dye molecules' stability under the conditions of light, heat, and chemicals leads to the fact that the dying effluents are difficult to degrade [1]. Many methods have been used to remove dyes from aqueous solutions, but adsorption has wide applicability for decolorization due to the economic system, high efficiency, eco-friendliness, and inactivity towards toxic substances [2].

Natural adsorbents such as agricultural waste, waste food, or inorganic materials have been the most popular for wastewater treatment due to their availability and low cost. Recently, Coal fly ash [3]., water hyacinth leaves [4], Moringa oleifera pod husk [5], bentonite [6], Tunisian clay [7], bentonite from Brazil [8], kaolin [9], and Perlite from Morocco [10] were used to remove dyes from dye solutions.

Perlite is an amorphous volcanic rock. Natural perlite is commonly grey, but can also be green, brown, blue, and red [11]. Its main constituents are silica and alumina. Silica and alumina can form the silanol and alumina hydroxide groups, which can bind adsorbates. Perlite is found in Lopburi and it can be used as a low-cost adsorbent. From the literature survey, it is found that the removal of magenta dye using perlite has not been reported. This work aimed to study the adsorption of a synthetic dye for silk yarn (magenta dye) onto Lopburi red perlite. The effects of adsorption, such as pH, contact time, initial dye concentration, and temperature were investigated. The experimental equilibrium data of adsorption were analyzed using the Langmuir and Freundlich isotherm models, and the experimental kinetic data were analyzed using pseudo-first, pseudo-second-order, and intraparticle diffusion at different temperatures. Also, the thermodynamic parameters such as ΔG, ΔH, and ΔS were determined.

2. Material and Methods
2.1 Preparation of adsorbent

The red perlite **(Figure 1.)** was collected from Sa Bot, Lopburi, Thailand. It was washed with distilled water and dried in a hot air oven at 100°C. Then it was powdered and sieved to a particle size of 150–300 mm. It was dried to a constant weight and stored in a desiccator for use.

Figure 1 Red perlite

2.2 Preparation of adsorbate

Adsorbate is a commercial synthetic dye for silk yarn. Its color is magenta, and its brand is "Cats run around the World" (Thailand). It was obtained from a local shop in Lopburi, Thailand. The dye was used without further purification. It was dried at 80°C for 2 h before use. The stock solution (500 mg/L) of dye was prepared by dissolving an accurately weighed quantity of dye in distilled water. The working solutions of the desired concentrations were obtained by dilutions with distilled water.

2.3 Characterization of adsorbent

The red perlite used in this study was characterized by Fourier transform infrared spectrometry (FTIR, Perkin Elmer, model two) and a Scanning electron microscope (SEM, LEO, model 1450 VP LEO). X-ray fluorescence spectrometry (XRF, HORIBA, model MESA-500W).

2.4 Determination of pHpzc

The point of zero charges (pH$_{PZC}$) was analyzed by the pH drift method. The pH was adjusted to a value between 2-12 by 0.1 M HCl and 0.1 M NaOH solutions. In the experiment, the adsorbent was dried in a hot air oven at 110°C for 3 h., and 0.1 g of adsorbent was taken in 50 ml of 0.1 M KNO$_3$ solution under agitation speed at room the

final pH was measured and plotted against the initial pH values.

2.5 Adsorption study

The adsorption study was performed in the batch method. For each experimental run, 100 ml of dye solution of known concentration was taken in a 250 mL Erlenmeyer flask containing 0.6 g of adsorbent. These flasks were agitated at a constant shaking rate of 200 rpm in a temperature-controlled orbital shaker (Vision Shaking Incubator, Model VS8480SRN) and maintained at 20, 30, and 40°C. At appropriate time intervals, each sample was withdrawn and filtered, and then the supernatant was measured for dye concentration by UV-visible spectrophotometer (Analytik Jena, Specord 210 plus) at 548 nm. The amount of the dye adsorption was calculated as Eq. (1):

$$q_t = \frac{(C_o - C_t)V}{W} \qquad (1)$$

where C_o (mg/L) is initial dye concentration, C_t (mg/L) is the concentration at any time, q_t (mg/g) is the amount adsorbed at any time, V(L) is the volume of the solution, and W(g) is the mass of adsorbent.

3. Adsorption Isotherm
3.1 The Langmuir isotherm

The Langmuir isotherm in a linear form is represented as follows [1]:

$$\frac{C_e}{q_e} = \frac{1}{q_{max}}C_e + \frac{1}{K_L q_m} \qquad (2)$$

where C_e (mg/L) is the equilibrium concentration, q_e (mg/g) is the amount adsorbed at equilibrium, K_L is the Langmuir constant, and q_{max} (mg/g) is the maximum adsorption capacity. The essential characteristics of the Langmuir isotherm can be expressed in terms of a dimensionless separation factor (R_L) which is defined by:

$$R_L = \frac{1}{(1 + K_L C_o)} \qquad (3)$$

3.2 The Freundlich isotherm

The Freundlich isotherm in a linear form is represented as follows [2]:

$$\log q_e = \log K_F + \left(\frac{1}{n}\right) \log C_e \qquad (4)$$

where K_F (L/g) is the adsorption capacity, and $\frac{1}{n}$ is the adsorption intensity.

4. Adsorption Kinetics
4.1 The pseudo-first-order model

The pseudo-first-order model in a linear form is written as follows [1]:

$$\log(q_e - q_t) = \log q_e - \frac{k_1}{2.303}t \qquad (5)$$

where k_1 (1/min) is the rate constant of pseudo-first, and q_t (mg/g) is the amount adsorbed at any time (min).

4.2 The pseudo-second-order model

The pseudo-second-order model is written in linear form as follows [1]:

$$\frac{t}{q_t} = \frac{1}{k_2 q_e^2} + \frac{1}{q_e}t \qquad (6)$$

where k_2 (g/(mg·min)) is the rate constant of the pseudo-second-order model.

4.3 The intraparticle diffusion model

The intraparticle diffusion model is expressed as Eq. (7):

$$q_t = K_{id}(t)^{1/2} + C \qquad (7)$$

where q_t is the amount of adsorbate retained at the time (t), K_{id} is the intraparticle diffusion rate constant (mg/(g·min$^{1/2}$), and C is the intercept.

5. Thermodynamic parameter of adsorption

The Gibbs free energy change (ΔG) in the adsorption process can be expressed as follows:

$$\Delta G = -RT \ln K_c \qquad (8)$$

where K_c ($K_c = q_e / C_e$) is the equilibrium constant, R is the gas constant and T is the absolute temperature. Also enthalpy (ΔH) and entropy (ΔS) changes can be estimated by the following equation:

$$\ln K_c = \frac{\Delta S}{R} - \frac{\Delta H}{RT} \qquad (9)$$

where ΔH and ΔS can be determined respectively by the slope and intercept of the linear plot between $\ln K_c$ and $1/T$.

6. Results and Discussion

6.1 Characterization

FTIR study

The adsorbent's functional group was observed using a Fourier transform infrared spectroscopy. The FTIR spectra of red perlite is shown in Figure 2. The spectra showed the presence of the following groups: O–Si–O stretching at 1009.9 cm⎕1, and the peak at 790.68 cm⎕1 corresponded to amorphous silica [12]

SEM study

Figure 3 represents the SEM of the red perlite surface. The micrograph showed the heterogeneous nature of surface morphology. The red perlite had a rougher and porous surface with random, widely distributed crevasses and pores of varying sizes. Its image is characterized by open pores, and the perlite used in this study is a good possibility for pore diffusion during adsorption [13].
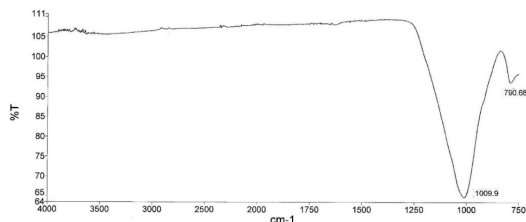

Figure 2 FTIR spectrum of red perlite

Figure 3 SEM of red perlite

XRF study

The red perlite used in this study was obtained from Sabot District, Lopburi, Thailand. By analyzing the adsorbent with XRF, the chemical compositions were SiO_2 (71.34%), Fe_2O_3 (4.26%), Al_2O_3 (11.13%), CaO (1.88%), K_2O (10.59%) and TiO_2 (0.801%). It can be seen that silica (SiO_2) and alumina (Al_2O_3) are the major compositions in the perlite, which is similar to Czech perlite [14]. Silica and alumina can form silanol and alumina hydroxide, which can bind the sorbates in the solution.

Point of zero charge (pH_pzc) of adsorbent

The pH of the zero point charge (pH_{pzc}) was *measured* by *pH drift method.* As seen in Fig. 4, the intersection plot shows the zero point charge at pH 3.5.
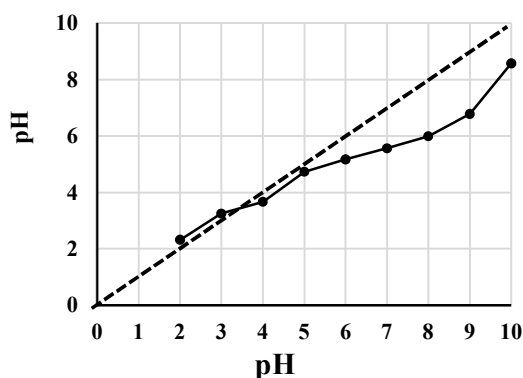

Figure 4 The pH at point of zero charge (pHpzc) of red perlite

6.2 Effect of pH

The adsorption of adsorbates from aqueous solutions is dependent on the solution's pH, which affects the surface charge of the adsorbent and degree of ionization. In the experiments, the effect of initial pH between 2-10 was investigated while the dye concentration temperature and contact time were fixed at 20 mg/L, 30°C, and 180 min, respectively. Figure 5 shows the percentage of adsorption versus pH. As seen in Figure 5, the percentage of adsorption increased with the increase of pH from 2 to 6. And, the maximum adsorption was obtained at pH 6. As the pH increased, the surface of the perlite gradually acquired a negative charge. As a result, the adsorption decreased and the percentage of adsorption was lower than pH 6. It was found that the pH value at the maximum adsorption was higher than the pH_{pzc} of perlite. At this condition, the surface charge of the adsorbent was negative. Therefore, the anionic dye could not be bound on the perlite surfaces due to the electrostatic interactions. However, the interactions could be hydrogen bonding [15]. Similar adsorption was reported for the adsorption of azo dyes [16].
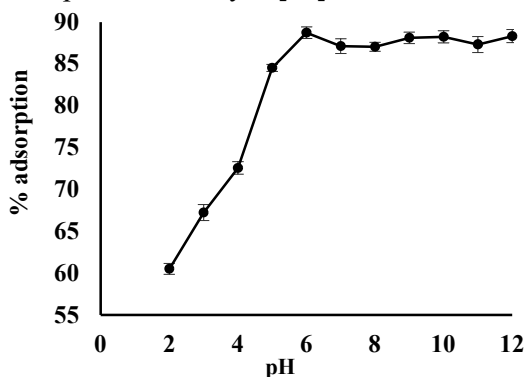
contact time at different temperatures are shown in Figure 6. The results showed that the adsorption capacity increased with the increase in contact time and temperature. The removal of dye was rapid in the initial stages of contact time and gradually decreased with time until equilibrium at 180 min.

The initial faster rate of adsorption may also be attributed to the presence of a large number of binding sites for adsorption, and the slower adsorption rate at the end is due to the saturation of the binding sites and attainment of equilibrium. A similar observation was reported for the adsorption of dye on natural untreated clay [9].

The effect of temperature was investigated at temperatures of 20, 30, and 40°C. The adsorption capacity values at equilibrium time were 2.90, 3.11, and 3.38 mg/g at 20, 30, and 40°C, respectively. The adsorption capacity increased with increasing temperature; thus, the adsorption was an endothermic process. This is because of the increasing mobility of the dye and an increase in the number of active sites for the adsorption process with increasing temperature [17].
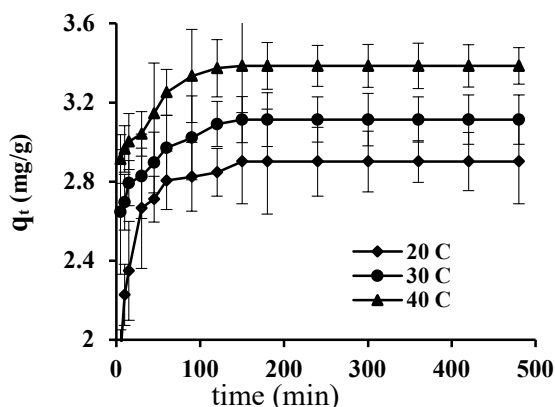

Figure 5 Effect of pH

Figure 6 Effect of contact time

6.3 Effect of contact time at different temperatures

The experiments were carried out to investigate the effect of contact time at three temperatures (20, 30, and 40°C) on the batch adsorption containing 100 mL of initial dye concentration of 20 mg/L and 0.6 g of perlite. The plots of adsorption capacity versus

6.4 Adsorption kinetic study

The adsorption kinetic data, obtained from section 6.2, were analyzed by the linear pseudo-first-order, pseudo-second-order, and intraparticle diffusion kinetic models. The calculated parameters were shown in Table 1. As seen in Table 1, the correlation

coefficients (R^2) of dye adsorption were 0.936, 0.882, and 0.942 for the pseudo-first-order model and 0.999, 0.999, and 0.999 for the pseudo-second-order model at 20, 30, and 40°C, respectively. Therefore, the kinetic data were fitted better with the pseudo-second-order model at all temperatures.

For the intraparticle diffusion study, the plots (not shown) between q_t versus $t^{1/2}$ were drawn, and the results showed three linear steps of the adsorption. The second linear step was the intraparticle diffusion of the adsorption. The values of the

intraparticle diffusion rate constant (K_{id}) were 0.072, 0.051, and 0.046 mg/g min$^{1/2}$ and the intercept (C) values were 1.881, 2.463, and 2.609 at 20, 30 and 40°C, respectively. The linear portions of the plots did not pass through the origin. This clearly showed that intraparticle diffusion was not the only rate-controlling step. Therefore, it might be concluded that surface adsorption and intraparticle diffusion were concurrently operating during adsorption

Table 1 Kinetic parameters of dye adsorption on red perlite at different temperature

Kinetic models	Temperature (°C)		
	20	30	40
q_e (exp) (mg/g)	2.901	3.113	3.385
Pseudo–first order			
q_e (cal) (mg/g)	1.095	1.550	1.154
k_1 (1/min)	0.021	0.018	0.025
R^2	0.936	0.882	0.942
Pseudo–second order			
q_e (cal) (mg/g)	2.933	3.138	3.409
k_2 (g/mg.min)	0.078	0.094	0.100
R^2	0.999	0.999	0.999
Intraparticle diffusion			
K_{id} (mg/g min$^{1/2}$)	0.072	0.051	0.046
C (mg/g)	1.881	2.463	2.609
R^2	0.901	0.941	0.887

6.5 Effect of initial dye concentration

The experiments were carried out to investigate the effect of initial dye concentration from 10 to 100 mg/L at three temperatures (20, 30, and 40°C) and equilibrium time (180 min). The adsorption capacities are shown in Figure 7. It revealed that the dye removal was concentration-dependent. The increase in initial dye concentration increased the adsorption capacity (q_e) of the dye. This may be due to the increase in driving the force of the

concentration gradient for mass transfer with the increase in initial dye concentration [18].

However, at higher concentration, the change of q_e versus initial dye concentration was decreasing. It can be explained that the adsorbent had a number of active sites, which became saturated at a certain concentration [19]. Moreover, at each dye concentration, the adsorption capacity increased when the adsorption temperature increased. Therefore, the adsorption was an endothermic process.
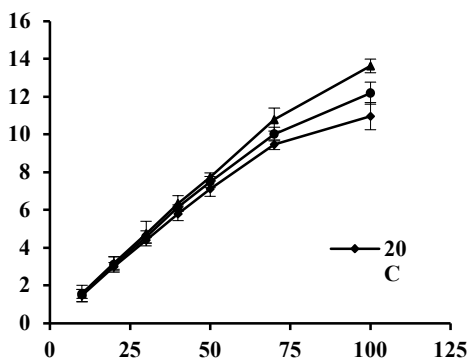
Figure 7 Effect of initial dye concentration

6.6 Adsorption isotherm study

From the results shown in Figure 6, the equilibrium adsorption data were plotted as the linear isotherm of the Langmuir and Freundlich models. The plots of the Langmuir isotherm at 20, 30, and 40 °C were shown in Figure 8. The values of the parameters from the linear plots of isotherms were calculated and tabulated in Table 2.

By considering to correlation coefficient (R^2) in Table 2, the results showed that the equilibrium data were better fitted to the Langmuir isotherm than the Freundlich isotherm at all temperatures. The adsorption isotherm indicated the homogeneous nature by the monolayer coverage of dye molecules onto red perlite surface and the maximum adsorption capacity (q_{max}) was 13.70, 14.71, and 16.63 mg/g at 20, 30, and 40°C, respectively.
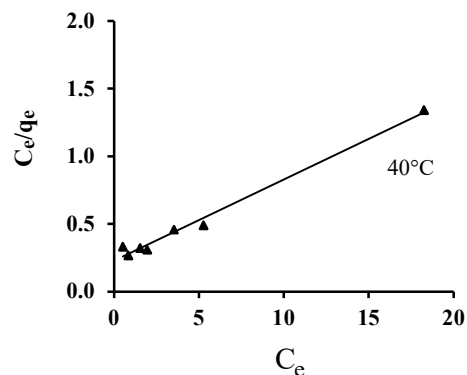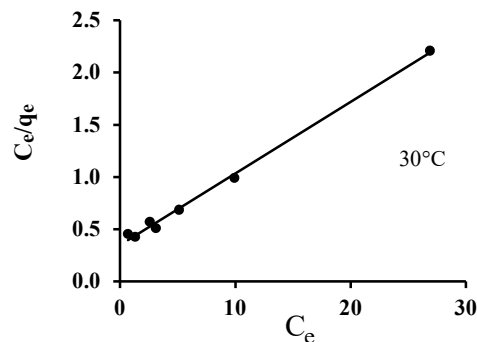

Figure 8 Langmuir isotherms at 20-40°C

The R_L values indicated the feasibility of the adsorption process because they were in the range of 0 and 1. A similar observation was reported for the adsorption of anionic dye on natural untreated clay [17].

From the Freundlich isotherm, the values of 1/n below 1 indicated a normal Langmuir isotherm and favorable adsorption [20]. The value of the Freundlich constant (K_F) represents the degree of adsorption. The K_F value increased with increasing temperature.
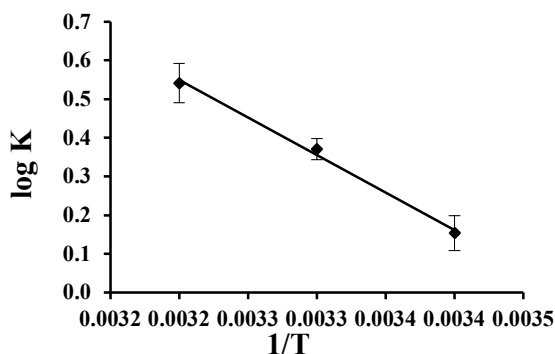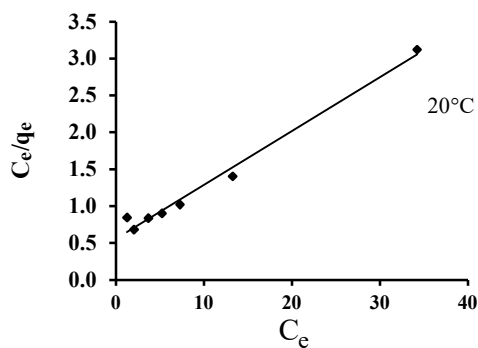

Figure 9 Thermodynamic of dye adsorption

Table 2 Isotherm parameters of dye onto red perlite

Isotherms	Temperature (°C)		
	20	30	40
Langmuir isotherm			
q_{max} (mg/g)	13.70	14.71	16.63
K_L (L/mg)	0.130	0.195	0.264
R_L	0.083–0.474	0.124–0.415	0.065–0.408
R^2	0.985	0.996	0.987
Freundlich isotherm			
K_F	1.82	2.55	3.35
1/n	0.591	0.558	0.586
R^2	0.896	0.913	0.893

6.7 Thermodynamic of adsorption study

The thermodynamic parameters such as the Gibbs free energy change (ΔG), enthalpy change (ΔH), and entropy change (ΔS) were determined. The experiments were carried out at three temperatures (20, 30, and 40 °C) on the batch adsorption containing 100 ml of 20 mg/L and 0.6 g of perlite at the equilibrium time. From the adsorption data, ΔG was calculated using Eq. (8). ΔH and ΔS were obtained from the slope and intercept of the plot (Figure 9.) between ln K_c ant 1/T. The values of ΔG, ΔH and ΔS were tabulated in Table 3.

As seen in Table 3, the free energy (ΔG) values of dye adsorption on perlite were −0.861, −2.15, and −3.24 kJ/mol at 20, 30, and 40°C, respectively. The negative values of ΔG indicated that the dye adsorption was spontaneous.

Table 3 Thermodynamic parameters for dye adsorption

Tem (K)	−ΔG (kJ/mol)	ΔH (kJ/mol)	ΔS (J/mol.K)
293	0.86	37.12	129.29
303	2.15		
313	3.24		

Table 4 Comparison of the dye adsorption capacity onto different adsorbents

The enthalpy change (ΔH) and entropy change (ΔS) of adsorption were 37.12 kJ/mol and 129.29 J/mol.K, respectively. In this study, a positive value of ΔH indicated the endothermic nature of the process, and a positive value of ΔS indicated the increasing randomness at the solid/liquid interface during the adsorption process.

In addition, E_a can be determined from the slope of the plot between ln k and 1/T (Figure 10). In this, k is the rate constant of pseudo-second-order kinetics, and the calculated E_a value of the adsorption is 4.45 kJ/mol, indicating that the adsorption is a physisorption process (E_a < 40 kJ/mol) [21]. The positive activation energy implies that the rate of adsorption increases with an increase in temperature, which leads to an increase in the probability of the colliding molecules being captured by the adsorbent. A similar result was reported by the adsorption of methylene blue dye on the O-CM-chitosan hydrogel [22]

| adsorbents	Class of dye	Dyes	Q_{max}, mg/g	References
Montmorillonite	Anionic	Magenta dye	161.0	[23]
HCl modified bentonite	Anionic	Methyl orange	47.8	[8]
bentonite	Anionic	Congo red	43.1	[6]
Perlite	Anionic	Congo red	55.5	[26]
Kaolin	Anionic	Congo red	5.4	[24]
Kaolin	Anionic	Reactive red	1.1	[9]
Lopburi red perlite	Anionic	Magenta dye	14.7	**This study**
Tunisian clay	Cationic	Crystal violet	86.5	[7]
Moroccan pyrophyllite	Cationic	Crystal violet	13.9	[25]
Kaolin	Cationic	Basic yellow 28	5.7	[9]
Pumice stone	Cationic	Crystal violet	6.99	[27]
Pumice stone	Cationic	Malachite green	22.6	[27]
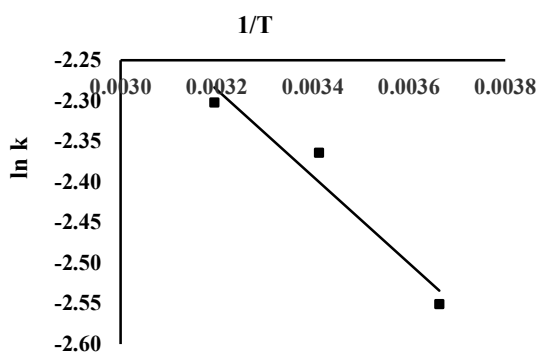
Figure 10 Arrhenius plot of dye adsorption

6.8 Comparative study of adsorption

In order to evaluate the efficiency of Lopburi red perlite used as a natural adsorbent in this study, a comparison based on the maximum adsorption capacity of dyes with different adsorbents is shown in Table 4. As seen in Table 4, the adsorption capacity is dependent on the class of dyes and the character of adsorbents. It is clear that the red perlite, used in this study, is indicative of the possibility to employ as an alternative low-cost adsorbent.

7. Conclusion

In this study, the adsorption of a synthetic dye for silk yarn onto red perlite was investigated. The red perlite was characterized by FTIR, SEM, and XRF. It contained mainly silica and alumina. The maximum adsorption of the dye occurred at pH 6 and at the equilibrium time (180 min). The kinetic adsorption data were better described by the pseudo-second-order model. The equilibrium adsorption results showed that the overall adsorption data were better fitted by the Langmuir isotherm at all temperatures, indicating the homogeneous nature of the monolayer coverage of dye on the red perlite surface. From the thermodynamic study, the adsorption was spontaneous and endothermic. The E_a value of the adsorption showed that the adsorption was a physisorption process. This study proved that red perlite could be used as a promising adsorbent for the removal of dye in water. Moreover, it can be concluded that the use of red perlite as an adsorbent could contribute not only to solving environmental problems but also to decreasing the overall cost of wastewater treatment.

Acknowledgment

References

[1] X. Han, X. Niu, and X.Ma, X. "Adsorption characteristics of methylene blue on poplar leaf in batch mode:

Equilibrium, kinetics and thermodynamics," *Korean Journal of Chemical Engineering*, vol.29, no.4, pp.494–502, Jan. 2012.

[2] D. Suteu, and T. Malutan, "Adsorption of cationic dye on cellolignin," *BioResources*, vol.8, no. 1, pp.427–446, Nov.2013.

[3] T. Rosa, A. Martins, M.T. Santos, T. Trindade, and N. Nunes, "Coal fly ash Waste, a Low-Cost Adsorbent for the removal of Mordant Orange Dye from Aqueous Media," *J. Braz. Chem. Soc.* vol. 32, no. 12, pp.2245-2256, 2021.

[4] Tttt I.G. Coronilla, L.M.Barrera, and E.C. Urbina, "Kinetic, isotherm and thermodynamic studies of amaranth dye biosorption from aqueous solution onto water hyacinth leaves," *Journal of Environmental Management*, vol.152, pp.99-108.

[5] A. Keereerak, and W. Chinpa, "A potential biosorbent from Moringa oleifera pod husk for crystal violet: Kinetics, isotherms, thermodynamic and desorption studies," *ScienceAsia*, vol. 46, pp.186-194, 2020.

[6] E. Rostami, R. Norouzbeigi, and A. R. Kelishami. "Thermal and chemical modification of bentonite for adsorption of an anionic dye," *Advances in Environmental Technology*, vol. 1, pp. 1-12, 2018.

[7] W. Hamza, N. Dammak, H.B. Hadjitaief, M. Eloussaief, M. Benzina, "Sono-assisted adsorption of Crystal violet dye onto Tunisian smectite clay: characterization, kinetics and adsorption isotherms," *Ecotoxicol Environ Saf*, vol. 163, pp. 365-371, 2018.

[8] Fernandes, J. V., Rodrigues, A. M., Menezes, R. R. & Neves, G. de A. 2020. Adsorption of Anionic Dye on the Acid-Functionalized Bentonite. Materials, 13(16), 3600.

[9] T.A. Aragaw, A.N. Alene, "A comparative study of acidic, basic, and reactive dyes adsorption from aqueous solution onto kaolin adsorbent: Effect of operating parameters, isotherms, kinetics,

and thermodynamics," *Emerging Contaminants*, vol. 8, pp. 59-64, 2013.

[10] H. Babas, G. Kaichouh, M. Khachani, M.E. Karbane, A. Chakir, A. Guenbour, A. Bellaouchou, I. Warad, and A. Zarrouk, "Equilibrium and kinetic studies for removal of antiviral sofosbuvir from aqueous solution by adsorption on expanded perlite: Experimental, modelling and optimization," *Surfaces and Interface*, vol.23, April. 2021.

[11] L. Meesuk, and S. Seammai, "The use of perlite to remove dark colour from repeatedly used palm oil," *ScienceAsia*, vol. 36, pp.33-39, 2010.

[12] C.A.P.Almeida, N.A. Debacher, A.J. Downs, L. Cottet, and C.AD. Mello, "Removal of methylene blue from colored effluents by adsorption on montmorillonite clay," *Journal of Colloid and Interface Science*, vol. 332, no 1, pp.46–53, April. 2009.

[13] A. Sar1, G. Sahinoglu, and M. Tuzen, "Antimony(III) Adsorption from Aqueous Solution Using Raw Perlite and Mn-Modified Perlite: Equilibrium, Thermodynamic, and Kinetic studies," *Industrial & Engineering Chemistry Research*, vol. 51, pp. 6877-6886, 2012.

[14] D.N. Thanh, M. Singh, P. Ulbrich, N. Strnadova, and F. Stepanek, "Perlite incorporating γ-Fe$_2$O$_3$ and α-MnO$_2$ nanomaterials: Preparation and evaluation of a new adsorbent for As(V) nanomaterials: Preparation and evaluation of a new adsorbent for As(V) removal," *Separation and Purification Technology*, vol. 82, pp.93-101, 2011.

[15] J. K. Komosinska, C.R. Dulewska, M. Pajak, I. Krzyzewska, and A. Dzieniszewska, "Adsorption of anionic dyes onto natural, thermally and chemically modified smectite clays," *Polish Journal of Chemical Technology*, vol. 16, no.4, pp.33-40, 2014.

[16] P. Sirajudheen, P. Karthikeyan, S. Vigneshwaran,, M.C. Basheer and S. Meenakshi, "Complex interior and surface modified alginate reinforced

reduced graphene oxide-hydroxyapatite hybrids: Removal of toxic azo dyes from the aqueous solution," *International Journal of Biological Macromolecules*. vol. 175, pp.361-371, April. 2021.

[17]   E. Errais, J. Duplay, M. Elhabiri, M. Khodja, M. Ocampo, R. Batenweck, R. Guyot, and F. Darragi, "Anionic RR120 dye adsorption onto raw clay: Surface properties and adsorption mechanism," *Colloids   and   Surfaces A:Physicochemical   and   Engineering Aspects,* vol.403, pp.69–78. June 2012.

[18]   A. El Kassimi, A. Boutouil, M. El Himri, M. Rachid Laamari, M. El Hadd, "Selective and competitive removal of three basic dyes from single, binary and ternary systems in aqueous solutions: A combined experimental and theoretical study," *Journal of Saudi Chemical Society*, vol.24, pp.524–544. May.2020.

[19]   M. Malakootian, and M.R.Heidari, "Reactive orange 16 dye adsorption from aqueous solutions by psyllium seed powder as a low-cost biosorbent: kinetic and equilibrium studies," *Applied Water Science*, vol.8, no.7, p.212, April.2018.

[20]   G.Ciobanu, S. Barna, and M. Harja, "Kinetic and equilibrium studies on adsorption of Reactive Blue 19 dye from aqueous solutions by nanohydroxyapatite adsorbent," *Archives of Environmental Protection*, vol. 42, no. 2, pp.3–11, 2016.

[21]   S.Chakraborty, A. Mukherjee, S. Das, N.R. Maddela, S. Iram, and P.Das, "Study on isotherm, kinetics, and thermodynamics of adsorption of crystal violet dye by calcium oxide modified fly ash," *Environmental   Engineering Research*, vol. 26, no. 1, pp.190372., March. 2020.

[22]   N.F Alharby, R.S. Almutairi, and N.A. Mohamed, "Adsorption Behavior of Methylene Blue Dye by Novel CrossLinked O-CM-Chitosan Hydrogel in Aqueous Solution: Kinetics, Isotherm and Thermodynamics," *Polymers*. vol.13, no. 21, pp.1-27, Oct. 2021.

[23]   A.S. Elsherbiny, "Adsorption kinetics and mechanism of acid dye onto montmorillonite from aqueous solutions: Stopped-flow measurements," *Applied Clay Science*, vol. 83-84, pp. 56-62, Oct. 2013.

[24]   V. Vimonses, S. Lei, B. Jin, C.W.K. Chow, C. Saint, "Adsorption of Congo red by three Australian kaolins," *Applied Clay Science*, vol. 43, no. 3-4, pp. 465-472, March. 2009.

[25]   Y. Miyah, A, Lahrichi, M. Idrissi, Sd. Boujrafc, H. Taouda, and F. Zerrouq , "Assessment of adsorption kinetics for removal potential of Crystal violet dye from aqueous solutions using Moroccan pyrophyllite," *Journal   of   the Association* of *ArabUniversities* for *Basic* and Applied Science. June . 2016.

[26]   G.   Vijayakumar,   M. Dharmendirakumar, S.Renganathan, S. Sivanesan, G. Baskar, and K. P. Elango, "Removal of Congo Red from Aqueous Solutions by Perlite," *Clean,* vol. 37, no. 4-5, pp. 355-364. 2009.

[27]   H. Shahesteha, A.B. Kelishamia, and R. Norouzbeigi, "Adsorption of malachite green and crystal violet cationic dyes from aqueous solution using pumice stone as a low-cost adsorbent: kinetic, equilibrium, and thermodynamic studies*, Desalination and Water Treatment*, pp. 1-10, 2015. DOI: 10.1080/19443994.2015.1054315